Available online at www.sciencedirect.com
ScienceDirect
Acta Materialia 59 (2011) 1162–1167
Acta MATERIALIA
www.elsevier.com/locate/actamat

The use of Larson–Miller parameters to monitor the evolution of Raman lines of tetragonal zirconia with high temperature aging

Andi M. Limarga [a,*], Justin Iveland [b], Molly Gentleman [c,1], Don M. Lipkin [c], David R. Clarke [a]

[a] School of Engineering and Applied Sciences, Harvard University, Cambridge, MA 02138, USA
[b] Materials Department, University of California, Santa Barbara, CA 93106, USA
[c] GE Research, Niskayuna, NY 12309, USA

Received 24 August 2010; received in revised form 5 October 2010; accepted 22 October 2010
Available online 12 November 2010

Abstract

The evolution of the Raman lines of metastable tetragonal yttria-stabilized zirconia with annealing for different times at different high temperatures has been monitored and the data analyzed using a Larson–Miller parameter. This normalization allowed the shift and sharpening of the Raman peaks of tetragonal zirconias having different stabilizer concentration and produced by different methods with different microstructures to be described by a common curve. The observed Raman shifts are consistent with evolution into a coherent mixture of tetragonal and cubic phases.

Keywords: Raman spectroscopy; Zirconia; High temperature aging

1. Introduction

In their studies of the effect of stress and temperature on the creep rupture time of gas turbine alloys, Larson and Miller showed that their results could be collapsed onto a common curve using a normalization of the form $LMP = T[C + \ln(t)]$ [1]. This normalization has been widely used since as a phenomenological method to relate the effects of time and temperature on various thermally activated processes. In this work we show that the Larson–Miller normalization can be employed to monitor changes in the Raman lines from yttria-stabilized zirconia as phase evolution occurs at high temperatures, in some instances before phase evolution is apparent by X-ray diffraction. This has important consequences for non-contact phase transformation studies as well as for condition assessment of zirconia-based coatings in high-temperature applications.

Tetragonal zirconia can only exist as a stable phase over a narrow range of high temperatures and yttria concentration (Fig. 1). The tetragonal phase is generally metastable with respect to their monoclinic and cubic polymorphs. Furthermore, while oxygen diffusion is very fast in yttria-stabilized zirconia – and is the basis for solid oxide fuel cells and oxygen sensors – cation diffusion is very slow. Consequently, equilibration of the tetragonal phase can take very long times, even at temperatures above 1000 °C [2]. These considerations are especially important for applications, such as thermal barrier coatings, which rely on the long-term, high-temperature stability of yttria-stabilized zirconia as well as its very low thermal conductivity. The optimum compositions for thermal barrier coatings have been found to be those shown in the grey box in Fig. 1 [3]. On prolonged high temperature exposure, these compositions, which are denoted tetragonal-prime, evolve into a mixture of the equilibrium cubic (yttrium-rich) and tetragonal (yttrium-poor) phases.

* Corresponding author. Tel.: +1 617 496 4295.
E-mail address: limarga@seas.harvard.edu (A.M. Limarga).
[1] Present address: Texas A&M University, College Station, TX 77843, USA.

1359-6454/$36.00 © 2010 Acta Materialia Inc. Published by Elsevier Ltd. All rights reserved.
doi:10.1016/j.actamat.2010.10.049

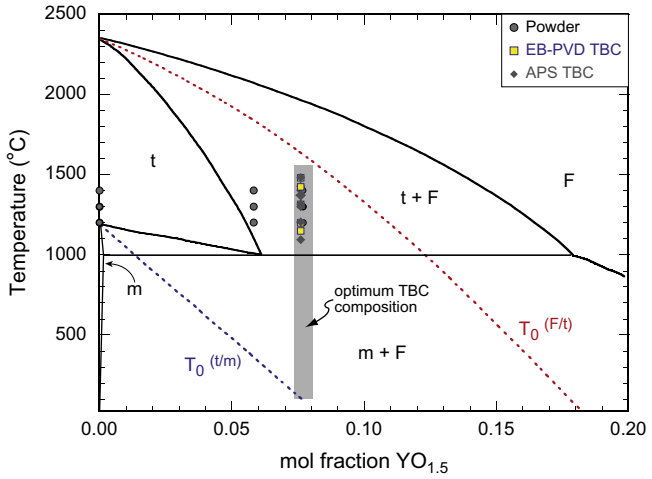

Fig. 1. Zirconia-rich portion of the ZrO_2–$YO_{1.5}$ phase diagram, showing the concentrations and aging temperatures used in this study. Both the equilibrium and metastable boundaries of the monoclinic, tetragonal and cubic phase fields are shown.

As part of a collaborative program investigating the phase evolution of tetragonal zirconia in thermal barrier coatings prepared by air plasma spraying (APS) and electron beam physical vapor deposition (EB–PVD), we have noticed that even before the onset of transformation to any monoclinic phase, the Raman peaks of tetragonal zirconia change with annealing at high temperatures. These observations, made on a series of zirconia powders and coatings after annealing for different times at different temperatures, are described in this work. We show that the changes in the peak position and peak width can be normalized using the Larson–Miller relation. Furthermore, the observed changes suggest that coherency strains arise during the initial stages of phase evolution.

2. Experimental details

2.1. Powders and coatings

Commercially available monoclinic and tetragonal zirconia powders with different concentrations of yttria (Table 1) were purchased from Tosoh Corp. (Tokyo, Japan). A variety of 7YSZ coatings (7 wt.% Y_2O_3 – stabilized ZrO_2) made by air plasma spraying (APS) and electron beam–physical vapor deposition (EB–PVD) were obtained from several sources, also listed in Table 1. The powders and coatings were annealed for different times and at different temperatures in air, as indicated Fig. 1. The heating and cooling rates varied from 10 °C min^{-1} (for heat treatment in a standard furnace) up to 300 °C min^{-1} (for annealing in a thermal cycling rig). As the Raman spectra from the as-received, nominally tetragonal Tosoh powders indicated that they were partially transformed to monoclinic, they were first all annealed at 1200 °C for 5 h. After this pre-treatment, all the powders except for the pure zirconia (0YS) were single-phase tetragonal.

Table 1
Composition of yttria-stabilized zirconia materials examined in this study.

Specimen	Designation[a]	mol.% $YO_{1.5}$	Phase
Powder	0YS	0	Monoclinic
Powder	3YS	5.8	Tetragonal
Powder	4YS	7.7	Tetragonal
APS	7YSZ	7.6	Tetragonal
EB–PVD	7YSZ	7.6	Tetragonal

[a] Designation of powder from Tosoh corresponds to the mol.% of Y_2O_3 in ZrO_2 while the convention used in thermal barrier coating applications is to refer to the concentration in wt.% of Y_2O_3 in ZrO_2.

2.2. Raman measurement and spectral analysis

Raman spectra were obtained from the coatings and powders using a LabRAM Aramis Raman system (Horiba Jobin Yvon, Edison, NJ) using the 633 nm excitation of a He–Ne laser operated at room temperature. The Raman spectra were acquired on a relatively large area, using a 10 μm diameter laser beam. Because of the translucency of zirconia and the sampling depth of collection optics, the spectra were obtained from a sufficiently large volume to encompass the statistical variations. The spectra recorded were subsequently deconvoluted using commercial peak-fitting software (GRAMS, Thermo Electron Corp., Philadelphia, PA) assuming mixed Lorentzian and Gaussian profiles for the Raman lines at 465, 610 and 640 cm^{-1}. The characteristic Raman lines of tetragonal zirconia at 145, 260 and 320 cm^{-1} are asymmetric and hence were fitted using a Breit–Wigner profile (an asymmetric Lorentzian function) [4] using the OriginPro package (OriginLab Corp., Northampton, MA). The peak positions were calibrated by also monitoring the laser Rayleigh line at 0 cm^{-1}.

3. Results

The Raman spectra of the monoclinic and tetragonal zirconia were consistent with prior reports and examples are shown in Fig. 2 as a function of annealing time and temperature. The positions and widths of the monoclinic peaks did not show any systematic change with either duration or temperature of annealing, as illustrated in Fig. 3. (The peak at around 103 cm^{-1} was selected because it has the most pronounced changes with aging compared to the other monoclinic peaks.)

By contrast, the tetragonal peaks shifted and narrowed with annealing time and temperature as illustrated by Fig. 4. For analysis, we selected three Raman peaks characteristic of the tetragonal phase, namely 145 cm^{-1} (E_g mode), 260 cm^{-1} (A_{1g} mode) and 465 cm^{-1} (E_g) because they have good intensities and are well isolated from other peaks, thereby minimizing errors associated with peak fitting and background subtraction. The mode assignment adopted in this work follow those proposed by Milman et al. [5] although other, older assignments have been pro-

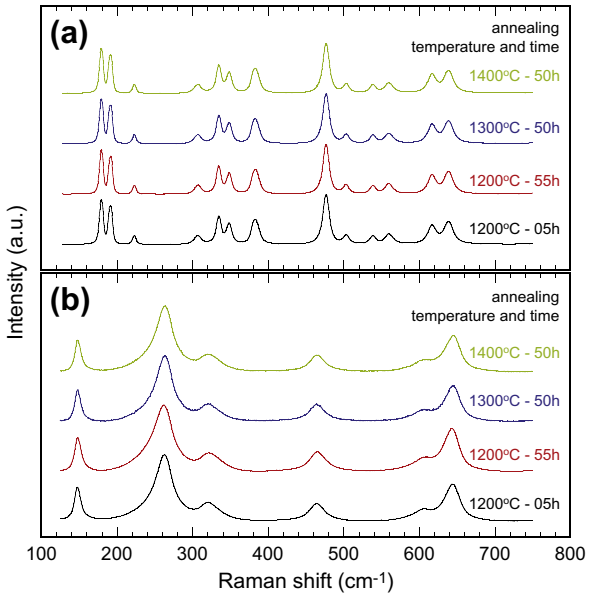

Fig. 2. Raman spectra of (a) monoclinic (0YS) and (b) tetragonal zirconia (3YS) powders after the different heat treatments indicated.

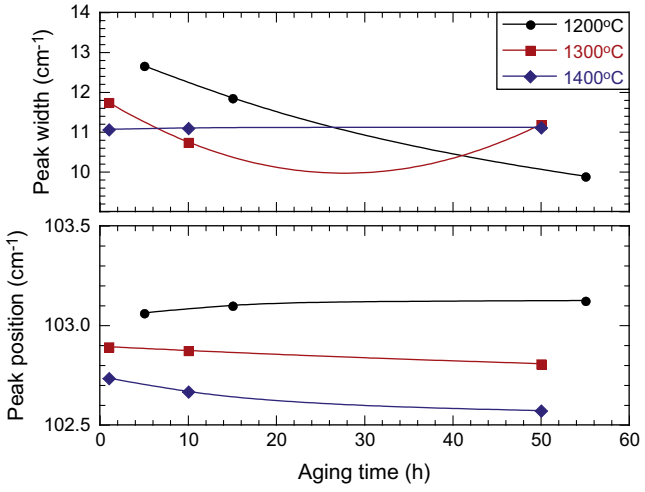

Fig. 3. Position and width of Raman peak of monoclinic zirconia at 103 cm^{-1} with aging. The error bars associated with the uncertainty in peak fitting are smaller than the symbols.

posed in the literature for the line at 260 cm^{-1} [6–8]. All the peaks undergo sharpening with annealing, consistent with the observation reported earlier on thermal barrier zirconia coating prepared by EB–PVD technique [4]. The peaks at 145 and 465 cm^{-1} shifted toward a smaller wave number while the peak at 260 cm^{-1} shifted toward a larger wave number. It is worth noting that such an opposite shift of the peak at 260 cm^{-1} was also observed in the study of temperature-dependent [9] and strain-dependent [10,11] Raman shifts. The peaks could not be deconvoluted into two separate peaks, which would be indicative of the presence of two distinct phases.

The differing behavior of the shifts and narrowing of the Raman peaks of tetragonal zirconia with annealing time and temperature are normalized using the Larson–Miller parameter, where T is temperature in Kelvin, t is the aging time in hours, and C is found to be 5, as shown in Figs. 5 and 6. Despite the different microstructures and yttria concentrations of the tetragonal zirconias investigated, the narrowing and the shift of the Raman peak position with LMP can be represented as a linear fit. The fitting results are listed in Table 2.

4. Discussion

The Raman results are discussed with the following questions in mind: (1) what is the origin of the observed value of the LMP parameter? (2) Why does the same LMP constant describe both the evolution of the FWHM and the shift of the tetragonal line even though the physical origin of line broadening and shift are usually unrelated? Consideration of these issues leads to the suggestion that the shift is associated with coherency strains developing as the tetragonal and cubic phases evolve from materials formed by highly non-equilibrium processes, such as plasma spraying and electron beam deposition, towards their equilibrium compositions.

The development of the Larson–Miller normalization starts with expressing the rate for a thermally activated process, r, as an Arrhenius type equation [1]:

$$r = A\exp(-Q/RT) \tag{1}$$

where A is the pre-exponential factor, Q is the activation energy, R is the universal gas constant and T is the temperature. Upon rearrangement, Eq. (1) becomes

$$Q/R = T[\ln(A) - \ln(r)] \tag{2}$$

As the rate, r, is inversely proportional to time, t, Eq. (2) can be further written as

$$Q/R = T[\ln(A) + \ln(t)] \tag{3}$$

Eq. (3) serves as the basis for the Larson–Miller parameter, LMP:

$$\mathrm{LMP} = Q/R = T[C + \ln(t)] \tag{4}$$

with the Larson–Miller constant defined as $C = \ln(A)$.

Our experimental data indicate that a value of $C = 5$ fits both the FWHM of the Raman lines as well as their shift. This is surprising at first but suggests that both are monitoring changes produced by the same diffusion mechanism. The FWHM of a Raman line is usually attributed to fluctuations in correlated phonon scattering caused by local atomic disorder, variations in isotopic concentration or variations in local strain. Consequently, the observed Raman line narrowing can be interpreted as a measure of local ordering as distinct to long-range rearrangements or diffusion. Formally, the width, ΔE, of a Raman line is related to the inverse of the lifetime, τ, of phonon scattering plus any instrumental broadening, ΔE_{inst}:

$$\Delta E = \frac{h}{\tau} + \Delta E_{inst} \tag{5}$$

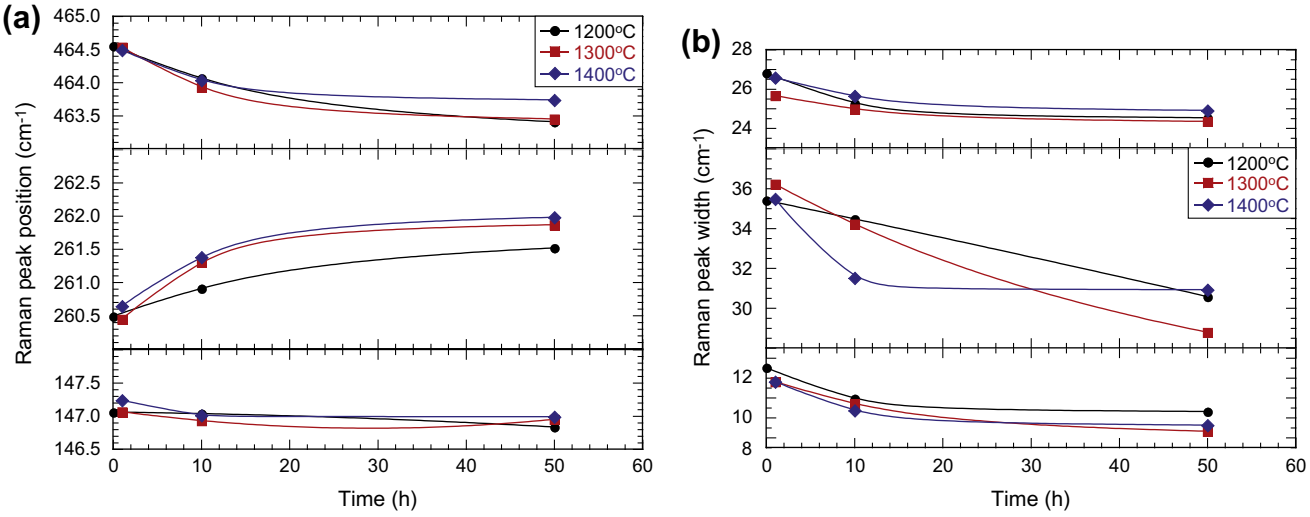

Fig. 4. Evolution of Raman peak of tetragonal zirconia powder (3YS) with aging: (a) peak position and (b) peak width. The error bars associated with the uncertainty in peak fitting are smaller than the symbols.

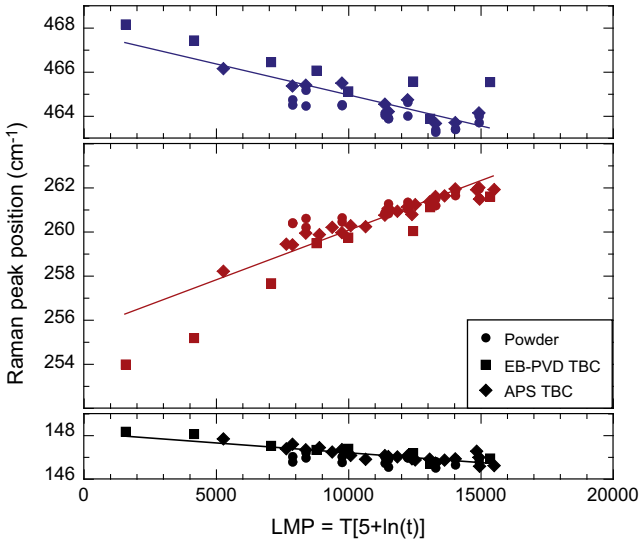

Fig. 5. Raman peak position of tetragonal zirconia with various compositions and microstructure as a function of Larson–Miller parameter.

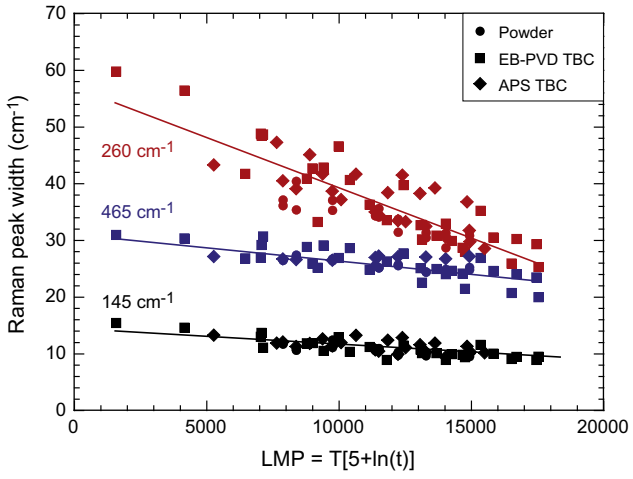

Fig. 6. Raman peak width of tetragonal zirconia with various composition and microstructure as a function of Larson–Miller parameter.

Compared to most simple oxides, the FWHM of the Raman lines of tetragonal zirconia are unusually large, much larger the instrumental broadening associated with our measurements and so the second term can be neglected. The phonon lifetime in a crystal containing defects, consists of two parts: the intrinsic lifetime associated with anharmonic phonon scattering, τ_A, and a defect-limited lifetime, τ_d associated with defect scattering of phonons:

$$\frac{1}{\tau} = \frac{1}{\tau_A} + \frac{1}{\tau_d} \tag{6}$$

The Raman modes in zirconia are primarily associated with vibrations of the oxygen sub-lattice so the defect-limited lifetime can be attributed to correlations between the oxygen vacancy concentrations such as suggested by Lughi and Clarke [4] and analyzed by Falkovsky [12]. As such, the narrowing of the Raman lines is due to an increase in the mean spacing of the oxygen vacancies, which, in turn, is associated with decreased local Y content in the tetragonal phase as it evolves. Although associated with local rearrangements, this process is assumed to be controlled by the same activation energy for long-range diffusion but our data provide no insight as to whether the rate-controlling step is yttrium ion diffusion or oxygen vacancy diffusion since the LMP normalization only indicates that the underlying process is thermally activated.

The systematic shift of Raman lines is normally associated with the development of lattice strains, changes in inter-atomic spacing induced by pressure or an external stress or mode softening. Since the same shifts are seen for both free-standing powders and for intact coatings on substrates it is unlikely that the shifts are due to externally imposed strains, such as might occur as a result of thermal

Table 2
Fitting parameters obtained for linear fits of Raman peak shift and peak width as functions of the Larson–Miller parameter.

	Raman band (cm^{-1})	Intercept (cm^{-1})	Slope (cm^{-1})
Position	145	148.1	-9.06×10^{-5}
	260	255.6	$+4.50 \times 10^{-4}$
	465	467.8	-2.81×10^{-4}
Width	145	14.4	-2.74×10^{-4}
	260	56.9	-1.77×10^{-3}
	465	30.9	-4.68×10^{-4}

expansion mismatch with a dissimilar substrate. More likely, the shifts are a result of internal mismatch strains generated as a result of the phase separation into a coherent mixture of cubic and tetragonal phases. The Raman signal from cubic zirconia is far weaker than that of tetragonal zirconia and there is considerable overlap between the strongest cubic line at ~610 cm^{-1} and the nearby tetragonal lines. Therefore, we cannot obtain any independent information on the cubic phase from the Raman spectra. Nevertheless, this limitation does not alter the interpretation that the observed shift in Raman lines is due to the evolution of misfit strains with aging. We note that the sign of the shift of the three Raman lines with LMP reduced time is opposite to the reported shift of the same Raman lines when polycrystalline tetragonal powder subject to hydrostatic compression [10]. It is also the same as the sign of the shifts when an uniaxial compression is applied to polycrystalline tetragonal zirconia [11]. Taken together with our observations, this suggests that the tetragonal phase is evolving under a tensional mean strain as phase separation proceeds. X-ray data taken from the literature of the lattice parameters of tetragonal zirconia as a function of aging time at 1450 °C indicate that the ratio of the lattice parameters (c/a) increases with aging time as the yttrium content in the tetragonal phase decreases [13]. As shown in Fig. 7, this literature data can be represented

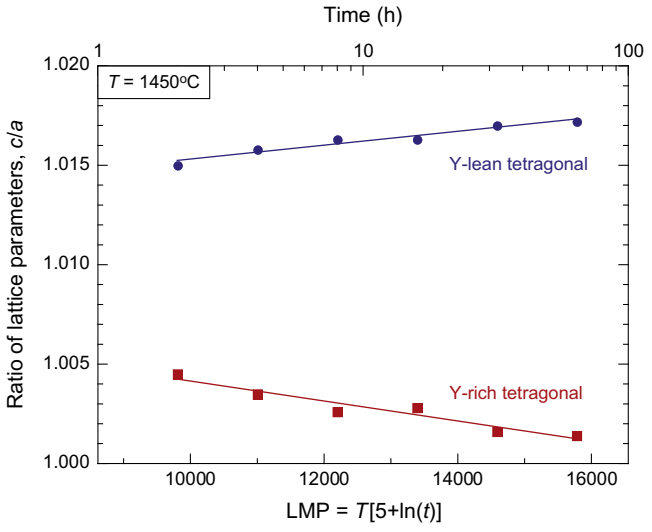

Fig. 7. Ratio of tetragonal lattice parameters as a function of Larson–Miller parameter with aging at 1450 °C (redrawn from Ref. [13]).

on a LMP reduced time with $C = 5$. The data are also consistent with the reported X-ray data of the lattice parameters of YSZ as a function of Y content indicating that the c/a ratio increases with decreasing Y content [14]. Furthermore, the volume of the tetragonal unit cell also decreases with decreasing Y content [14]. Taking into account these facts, our Raman shifts can be interpreted as a result of yttrium ions and oxygen vacancies rearranging to form, concurrently, local tetragonal and cubic phases in a two-phase composite whose average stress is zero. Thus, as the tetragonal and cubic phases evolve the cubic phase will be under average compression and the tetragonal phase will be under average tension on account of their different yttrium concentrations. As aging continues, the yttrium concentration decreases in the tetragonal and increases in the cubic phases. Because the Raman spectra were obtained from a large number of polycrystalline grains, the shifts are related to the mean strain, namely $\varepsilon_{ii} = (\varepsilon_{11} + \varepsilon_{22} + \varepsilon_{33})$ and can be compared to the shifts measured under hydrostatic pressures by Bouvier and Lucazeau [10] and for polycrystalline zirconia under compression by Limarga and Clarke [11]. (The literature measurements are presented in terms of stress, so must be divided by the bulk modulus, K, of zirconia, 200 GPa, to obtain the mean strain.) Assuming that the strain is zero before aging, the mean strain can be estimated as the tetragonal phase evolves. For instance, taking the shift of the 260 cm^{-1} line from Fig. 5 as an example, after an LMP value of 15,000 the strain in the tetragonal phase is $\sim 1.9\ \text{GPa}/K \approx 0.01$. This value is the sum of the misfit strain and any thermal expansion mismatch strain. The latter is not known with any precision since the strain-free lattice parameters as a function of temperature are unknown.

Although the Raman results do not provide any insight into the morphological evolution of the phases, we emphasize that our results are consistent with coherent phase separation as distinct from a nucleation and growth process. In phase evolution by nucleation and growth, the compositions of the precipitating phases do not change after nucleation and while the nucleating phases remain coherent with the matrix, strains develop but they do not increase as growth continues. Furthermore, away from the nucleated phases, the "matrix" does not significantly change in composition. So, if both tetragonal and cubic phases nucleate from the tetragonal-prime phase, one would expect some signal to persist from the tetragonal-prime phase. This is not observed and, as mentioned earlier, the Raman lines cannot be deconvoluted into two separate tetragonal phases. The suggestion that the phase separation within the metastable tetragonal region of the yttria-stabilized zirconia is coherent is not entirely new but data supporting it have not previously been presented. It was first proposed by Hillert and Sakuma, who considered the tetragonal–cubic phase separation in yttria-stabilized zirconia in the form of spinodal decomposition [15,16]. The observation that the same LMP value describes the Raman shift as the Raman line narrowing further suggests that both the

oxygen vacancy rearrangements associated with the phase separation and the lattice strains are determined by the same rate controlling thermal activation process. In view of the fact that oxygen vacancy diffusivity is so large and the phase evolution occurs over hundreds of hours above 1200 °C, it is highly likely that the rate-controlling step is the diffusion of yttrium ions but as mentioned earlier the value of the LMP parameter provides no insight as to the mechanism.

Lastly, the results obtained in this study have implications for the measurement by Raman spectroscopy of temperatures and strains in coatings and components, such as biomedical implants and teeth, made of tetragonal zirconia. Both measurements rely on the Raman peak shift from a reference position to estimate the temperature [9,17] and the strain in the material [18–21]. As shown in this study, the Raman peak positions shift with aging, hence they have to be calibrated in order to perform either temperature or strain measurement. It was shown previously that this type of correction is necessary in the residual strain measurement using Raman spectroscopy on plasma-sprayed tetragonal zirconia subjected to a thermal gradient [22].

5. Conclusion

The evolution of Raman lines of tetragonal zirconia with aging at various temperatures and duration has been evaluated using the Larson–Miller relation. It was found that the shift and sharpening of Raman lines of tetragonal zirconia with various yttria stabilizer contents and various microstructures can be collapsed onto a common curve using a Larson–Miller constant of 5. This suggests that both the oxygen vacancy rearrangements associated with the phase separation and the lattice strains are determined by the same rate controlling thermal activation process. The sharpening of Raman lines is attributed to the increase spacing between oxygen vacancies due to the decrease of local Y content in the tetragonal phase. Finally, it is proposed that the shift of the Raman peaks with aging is caused by the internal mismatch strain due to phase separation from the metastable tetragonal-prime into a coherent mixture of yttrium-poor tetragonal and yttrium-rich cubic phases.

Acknowledgements

The authors would like to thank Dr. Ken Murphy of Howmet Corporation for the EB–PVD samples, Mr. Warren Nelson and Drs. Curt Johnson and Wayne Hasz for the APS samples and invaluable discussions. This work was supported by the National Science Foundation under FRG-GOALI Contract NSF/DMR0605700. The work at GE was supported by the US Department of Energy via Cooperative Agreement DE-FC26-05NT42643. Any opinions, findings, conclusions or other recommendations expressed are those of the authors and do not necessarily reflect the views of the US Department of Energy or the National Science Foundation.

References

[1] Larson FR, Miller JA. Trans ASME 1952;74:765.
[2] Chevalier J, Gremillard L, Virkar AV, Clarke DR. J Am Ceram Soc 2009;92:1901.
[3] Stecura S. Optimization of the NiCrAl–Y/ZrO_2–Y_2O_3 thermal barrier system. NASA-TM 86905; 1985.
[4] Lughi V, Clarke DR. J Am Ceram Soc 2005;88:2552.
[5] Milman V, Perlov A, Refson K, Clark SJ, Gavartin J, Winkler B. J Phys: Condens Matter 2009;21:485404.
[6] Freiberg A, Perry CH. J Phys Chem Solids 1981;42:513.
[7] Bouvier P, Gupta HC, Lucazeau G. J Phys Chem Solids 2001;62:873.
[8] Rignanese G-M, Detraux F, Gonze X, Pasquarello A. Phys Rev B 2001;64:134301.
[9] Lughi V, Clarke DR. J Appl Phys 2007;101:053524.
[10] Bouvier P, Lucazeau G. J Phys Chem Solids 2000;61:569.
[11] Limarga AM, Clarke DR. J Am Ceram Soc 2007;90:1272.
[12] Falkovsky LA. J Exp Theor Phys 2006;102:155.
[13] Cairney JM, Rebollo NR, Ruhle M, Levi CG. Int J Mater Res 2007;98:1177.
[14] Yashima M, Sasaki S, Kakihana M, Yamaguchi Y, Arashi H, Yoshimura M. Acta Crystallogr 1994;B50:663.
[15] Hillert M. J Am Ceram Soc 1991;74:2005.
[16] Hillert M, Sakuma T. Acta Metall Mater 1991;39:1111.
[17] Gentleman MM, Lughi V, Nychka JA, Clarke DR. Int J Appl Ceram Technol 2006;3:105.
[18] Teixeira V, Andritschky M, Fischer W, Buchkremer HP, Stover D. J Mater Process Technol 1999;92–93:209.
[19] Portinha A, Teixeira V, Carneiroa J, Beghi MG, Bottani CE, Franco N, et al. Surf Coat Technol 2004;188–189:120.
[20] Tomimatsu T, Kagawa Y, Zhu SJ. Metall Mater Trans A 2003;34A:1739.
[21] Tanaka M, Hasegawa M, Dericioglu AF, Kagawa Y. Mater Sci Eng A 2006;419:262.
[22] Limarga AM, Vassen R, Clarke DR. J Appl Mech 2011;78:011003.